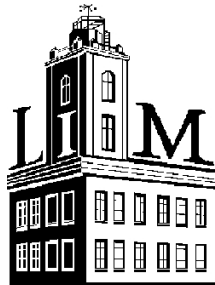


University of Leipzig
Faculty of Physics and Earth Sciences
Leipzig Institute of Meteorology



The 2020 Siberian heatwave in connection to the middle atmosphere in MUAM

Elaboration
Modul Dynamics of Middle Atmosphere
Winter semester 2020/21

submitted by:
Anton Kötsche
Matriculation number: 3719953
08.03.2020

Contents

1	Introduction and Motivation	III
2	Data and Methods	IV
3	The 19/20 stratospheric polar vortex	V
3.1	Zonal wind anomalies	V
3.2	Wave driving	V
3.3	NAM and AO	VIII
4	Results	X
	Literatur	XI
	Abbildungsverzeichnis	XIII

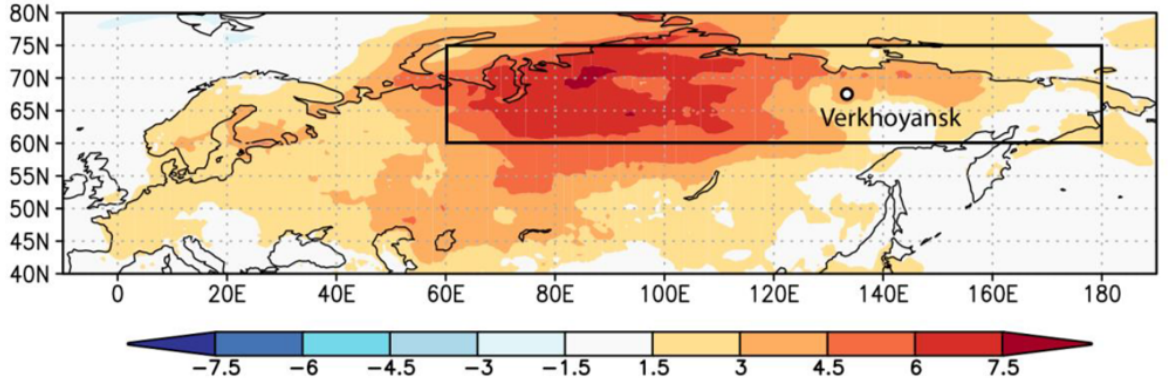


Figure 1: *ERA5 near surface temperature (T_{2m}) anomalies [$^{\circ}C$] for Jan-Jun 2020. Reference period: 1981-2010. Cited from Ciavarella et al. (2020).*

1 Introduction and Motivation

During northern-hemisphere (NH) winter, the principal circulation feature of the stratosphere is the stratospheric polar vortex (SPV). This strong westerly circulation from 100 hPa to above 1 hPa roughly spans between 30°N - 60°N. During NH winter, the SPV strengthens via radiative cooling. Its strength is also modulated by dynamical troposphere-stratosphere coupling via planetary waves generated in the troposphere [e.g., Charney and Drazin, 1961]. Waves from the troposphere travel vertically into the stratosphere where they brake. That delivers easterly momentum which disturbs the westerly circulation of the SPV, causing stratospheric warming. The seasonal strength of the SPV therefore depends on the wave driving of the stratosphere [Lawrence et al., 2020]. Processes like downward wave coupling events, where upward travelling waves are reflected by the stratosphere, also add to strengthen the SPV [Dunn-Sigouin and Shaw, 2015; Shaw and Perlwitz, 2014]. The NH SPV of 2019/2020 was one of the coldest and strongest ever recorded. During the whole winter, it remained almost undisturbed due to unusually low wave activity from the troposphere. Waves that did travel upward from the stratosphere mostly got reflected, resulting in downward wave coupling events which further added to strengthen the SPV [Lawrence et al., 2020].

The strength of the polar vortex has a close statistical relationship to the phase of the Arctic Oscillation (AO) [Kidston et al., 2015]. The AO is characterized by sea-level pressure (SLP) anomalies of the Arctic and regions between 37-45°N. Anomalously low SLP over the arctic and high SLP over the subtropics leads to a positive AO. The Northern Annual Mode (NAM) takes the meridional shifts of mass into or out of the polar cap throughout the atmospheric column into account.

A strong or weak SPV corresponds with a positive or negative phase of the NAM. These positive or negative phases of the NAM in the stratosphere are usually followed by equally negative or positive phases of the AO in the troposphere [e.g., Baldwin and Dunkerton, 2001; Domeisen, 2019; Dunn-Sigouin and Shaw, 2015; Kidston et al., 2015].

The persistent strength of the 2019/2020 SPV was accompanied by a persistent positive Phase of the Arctic Oscillation (AO). Lawrence et al. (2020) stated, that this was consistent with large parts of the observed temperature and precipitation anomalies throughout the season. The most noticeable anomaly that gained international interest was the so called Siberian heatwave. As shown in figure 1 by Ciavarella et al. (2020), 2 m temperature anomalies from January to June 2020 exceeded 6°C all over Siberia. An all time temperature record of 38°C was reached in the Arctic Circle at the town of Verkhonjansk [Overland and Wang, 2020]. The Siberian heatwave caused melting permafrost, large wildfires, oil spillings and insect plagues [Ciavarella et al., 2020].

The confluence of atmospheric conditions in connection to this extreme event is a prime example of the two-way coupling between troposphere and stratosphere.

2 Data and Methods

The 2019/2020 SPV shall be further analysed by using the Middle and Upper Atmosphere Model (MUAM), which is based on the Cologne Model of the Middle Atmosphere. The model was developed by the Leipzig Institute for Meteorology in cooperation with the RSHU in St. Petersburg. It is a nonlinear mechanistic 3D grid point model of neutral atmospheric circulation, which features 56 height layers up to 160 km log-p-height. It has a latitude resolution of 5° and a longitude resolution of 5.625° .

The dynamics are described by the primitive equations in flux form on a sphere under hydrostatic assumption. The Matsuno-Integration scheme is used for time integration. Energy conversions through turbulent mixing, ion drag and molecular heat conduction are included [Froelich and Jacobi, 2004]. In the lower atmosphere (up to 30 km), the model is driven by reanalysis data of mean zonal temperature (NCEP- or ERA-Interim reanalysis data). A nudging term is used and the model is adjusted to fit tropospheric model output in these lower levels [Lilienthal et al., 2016].

For this study, a very basic version of MUAM is used to compute monthly means of different quantities throughout the atmosphere such as wind, geopotential or temperature. As stated in Pogoreltsev et al. (2007), solar tides in the model are created directly by the absorption radiation. An enclosing radiation routine characterises absorption and emission processes for the important gases of the middle atmosphere [Froelich and Jacobi, 2004]. Stationary and travelling planetary waves are introduced at the lower boundary. For stationary waves, 11-year averaged assimilated data is used and included into the geopotential height field at 1000 hPa. Travelling Rossby and Kelvin waves are included by calculating the Hough functions. Those waves are then added to the geopotential height field as well [Pogoreltsev et al., 2007]. Further details can be found in Pogoreltsev et al. (2007) or Froelich et al. (2003).

For this study, the first three months of 2020 are considered. Anomalies for every month are based on the 2008-2018 means, also calculated by MUAM. Eliassen Palm (EP) fluxes are computed and used to describe the wave driving conditions. Output of MUAM is compared with MERRA 2 Output. The MERRA 2 Output was visualized by Lawrence et al. (2020).

3 The 19/20 stratospheric polar vortex

3.1 Zonal wind anomalies

Figure 2 shows MERRA-2 data of the zonal mean zonal wind anomalies in 10hPa depend on the latitude and in 60°N as function of pressure. It's cited from Lawrence et al. (2020). For almost the entire season, the SPV winds were above average between 55°N - 75°N and 100 hPa - 1 hPa. While winds were partly below average in early December, the SPV became stronger in January. Winds were more than 20 m/s higher than those in the climatology. After a small disturbance in early February, the SPV winds exceeded 2 standard deviations of the climatology and reached a MERRA-2 all time record. The SPV remained that strong until April, where it slowly started to weaken, yet still being stronger than climatology average. Winds in the upper stratosphere and lower mesosphere (USLM) showed quite the opposite. Windspeeds above 1 hPa were very strong in mid December, but generally weaker than normal after early January.

Looking at monthly mean zonal wind anomalies calculated by MUAM (figure 3), it's obvious they won't be quite as detailed. Negative anomalies in the USLM are not visible as they are in MERRA-2 data. The anomalies are in general lower than those in figure 4, but that might also be due to different reference periods. Anomalies below 10 hPa are higher and somewhat match the MERRA-2 data better in terms of temporal distribution of maxima (highest anomaly in March). That is most likely caused by the nudging term in the lower levels, which adjusts the model output to fit reanalysis data.

3.2 Wave driving

As mentioned before, waves generated in the troposphere can travel into the stratosphere and disturb the polar vortex. To quantify wave driving, the EP flux and its divergence is calculated. Figure 4 shows the EP flux and its divergence calculated from MUAM data in February 2020. Upward travelling waves or downward reflection events are usually short lived and transient [Lawrence et al., 2020]. So rather than actual events, the monthly mean shows a snapshot of what processes dominate in this timespan. The zonal windfield shows a split-jet structure with a high latitude maximum roughly between 40 km - 60 km and a low level subtropical jet maximum. MUAM simulates large wave activity in the troposphere between 40°N and 70°N, shown by upward pointing EP flux arrows and strong EP divergence. In the vicinity of the tropopause, waves are directed equatorward, where they dissipate or are directed back into the tropopause. In the stratosphere, no

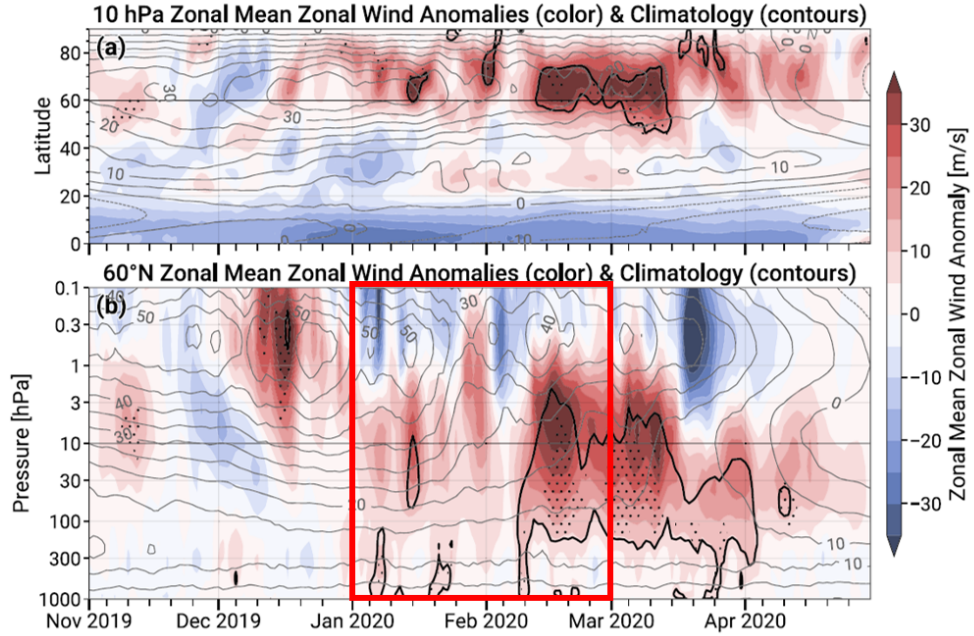


Figure 2: Time series of zonal mean zonal wind anomalies as a function of latitude at 10 hPa (a) and at 60°N as a function of pressure (b). The gray line contours represent the climatology; the black lines enclose the times when anomalies exceed +2 standard deviations of the November–April daily climatology; and stippling indicates when the zonal wind values were maxima in the MERRA-2 record. Cited from Lawrence et al. (2020). The red box in both figures was added later and marks the height and time spans both figures show to make comparison easier.

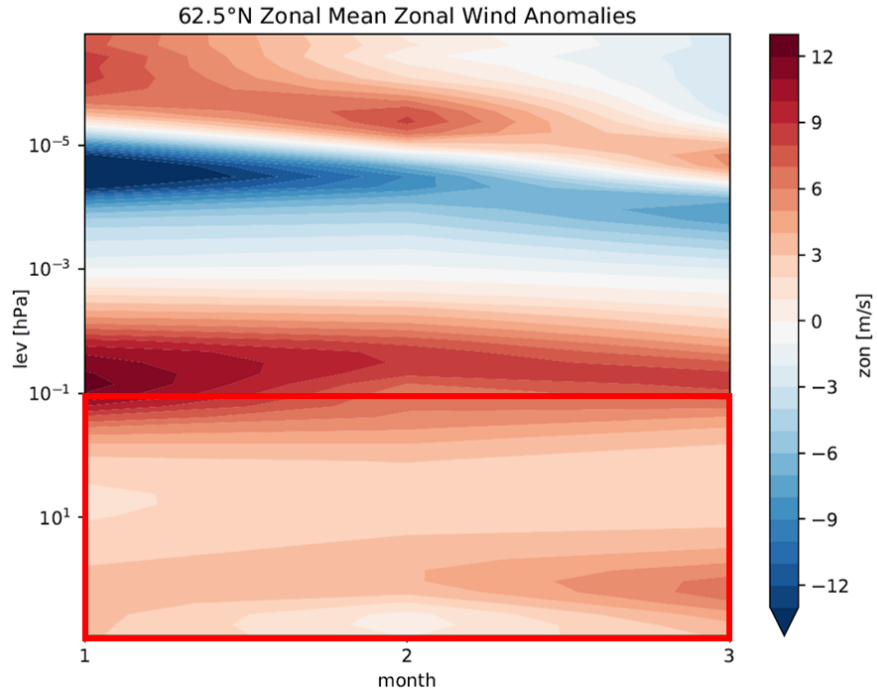


Figure 3: Monthly zonal mean zonal wind anomalies JFM 2020 based on the JFM 2008–2018 means. Computed with MUAM.

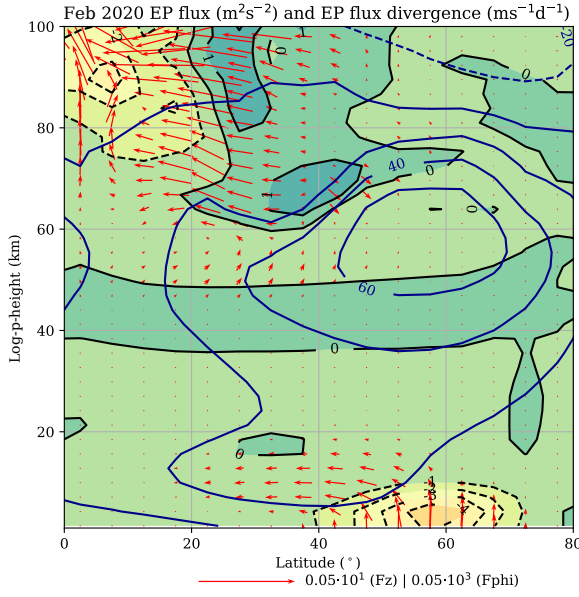


Figure 4: *EP flux (red arrows) and its divergence (contours) of February 2020 as function of pressure and latitude, calculated with MUAM. Blue lines show the mean zonal wind in m/s.*

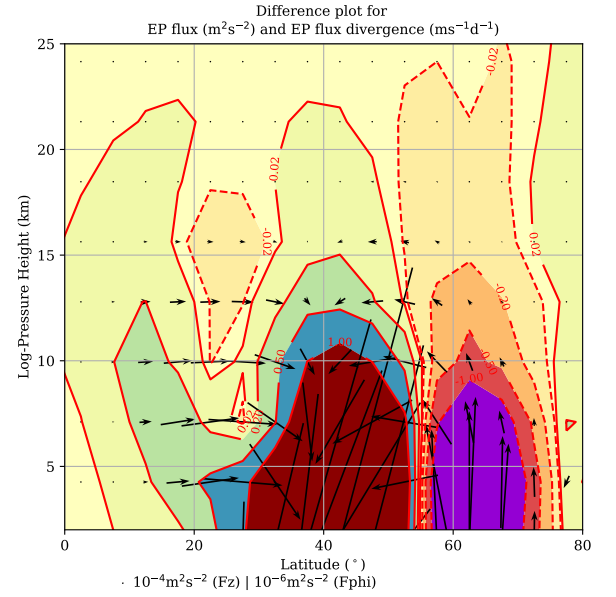


Figure 5: *EP flux anomalies (red arrows) and its divergence anomalies (contours) of February 2020 as function of pressure and latitude. Reference period is the 2008-2018 February mean.*

wave activity is present and the SPV therefore remains undisturbed. Wave activity in the middle and upper mesosphere is more pronounced, especially south of 50 °N. Figure 2 shows some disturbances of the SPV in early February, these wave interactions of the SPV with mesospheric circulations could be the cause. Lawrence et al. (2020) stated, that this configuration of the two jet maxima has shown to be highly reflective for stationary wave number 1. Waves are meridionally confined and vertical wave propagation is inhibited by the strong SPV and the low level subtropical jet.

Figure 5 shows the EP flux and divergence anomalies in February 2020. There is a higher than usual amount of waves travelling upward from the lower troposphere. Waves are hindered to travel toward the equator and into the stratosphere as they would usually do. This is shown by the poleward and downward pointing arrows between 20 °N and 55 °N. The MUAM Output agrees with the statement of Lawrence et al. (2020) and indeed shows, that this split jet configuration confines upward and meridional wave propagation.

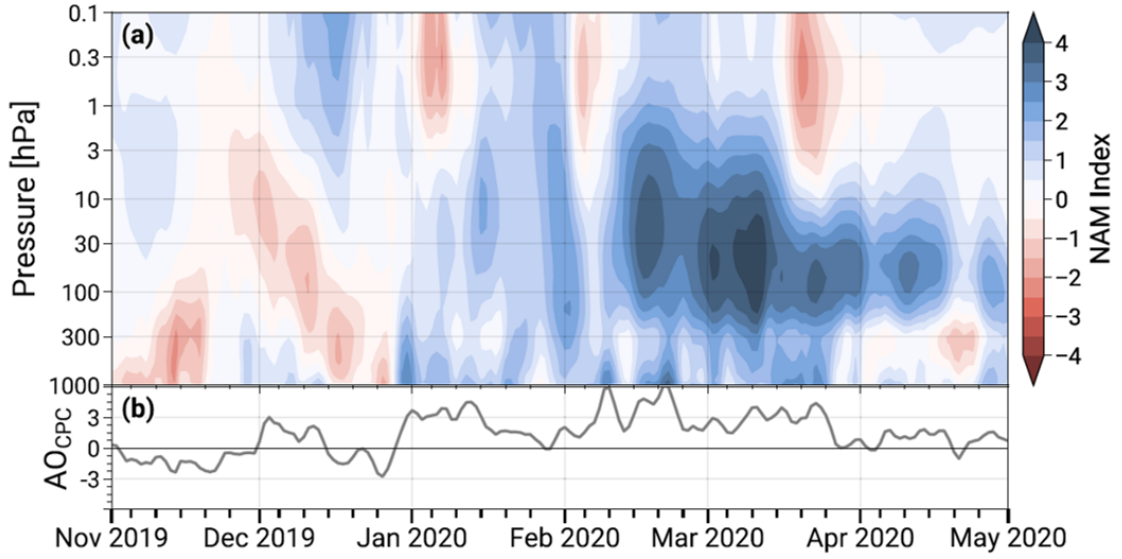


Figure 6: *Time series of the Northern Annular Mode (a) and CPC Arctic Oscillation (b) indices from November 2019 through April 2020. Cited from Lawrence et al. (2020).*

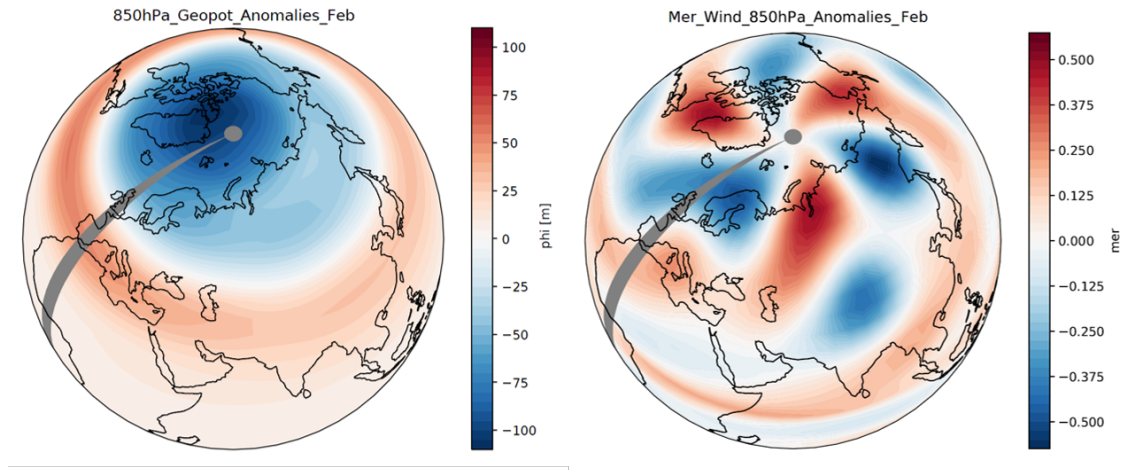


Figure 7: *850 hPa geopotential height anomalies (left) and 850 hPa meridional wind anomalies (right) in February 2020, calculated with MUAM. Reference periode was 2008-2018.*

3.3 NAM and AO

It was not possible to calculate useful AO or the NAM from the MUAM data used in this study. Hence, only the data plotted by Lawrence et al. (2020) in figure 6 can be used. Except a small disturbance in mid December, the AO remained locked in a positive phase throughout JFM 2020. Especially in February and March, the positive tropospheric AO correlates with a strongly positive NAM. That indicates, that the stratospheric zonal wind pattern also extended into the troposphere [Lawrence et al., 2020].

The positive AO can be equated with anomalously low sea level pressure over the arctic and anomalously high pressure over the subtropics, paradigmatically shown by the geopotential height in 850 hPa in (figure 7 left). Lawrence et al. (2020) have shown that the correlation of stratospheric NAM and polar cap sea level pressure (SLP) is statistical significant at a 99% level. Because the AO remained positive for such a long time, also the constellation of pressure systems barely changed. That way, the vertical connection of SPV and tropospheric jet stream from January–April 2020 provided the atmospheric dynamic feature that supported northward advection of warm airmasses [Overland and Wang, 2020]. This is exemplary shown in figure 7 right, where the meridional wind anomalies in 850 hPa show positive values, meaning a stronger than usual poleward advection of airmasses. The enhanced northward advection of airmasses was, as Overland and Wang (2020) stated, the main reason for the anomalously high temperatures in Siberia between January and April. The direct connection to the highly positive AO is illustrated in figure 8. The temperature anomalies of JFM 2020 (figure 8 a) fit the expected anomalies congruent with the AO (figure 8b) very accurate. The congruent values are determined from multiplying the 2020 JFM AOCPC value with the regression map of these quantities onto the JFM AOCPC historical time series [Lawrence et al., 2020]. Surface temperatures were anomalously high over whole Eurasia and anomalously cold over Canada, Greenland and Alaska. Referring to Lawrence et al. (2020), the JFM AO explains about two thirds of the amplitude of observed temperature anomalies.

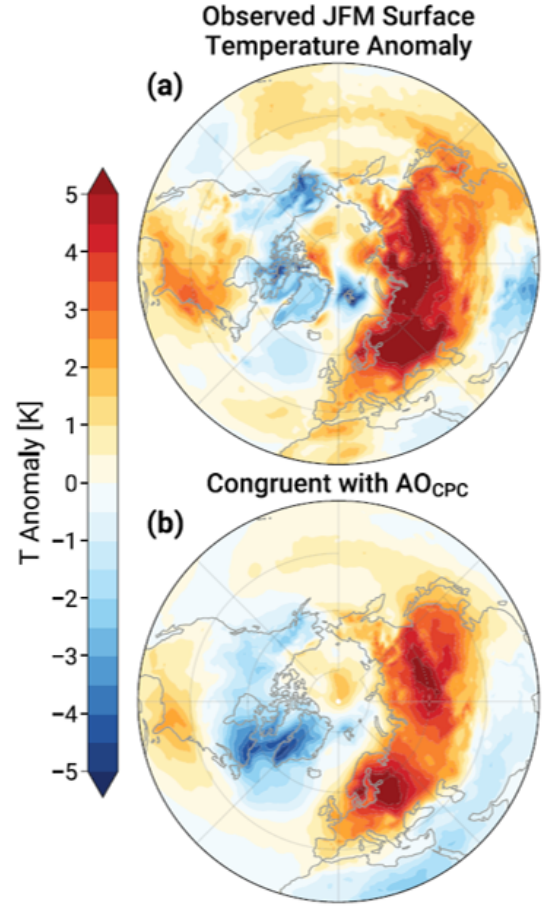


Figure 8: Maps of the observed January–March (JFM) 2020 anomalies in surface temperature (a), and the anomalies congruent with the JFM AOCPC (b). Cited from Lawrence et al. (2020).

4 Results

The 2019/2020 NH SPV was the strongest on record since 1979/80 and the strongest ever recorded in 100 hPa [Lawrence et al., 2020]. Its strength was gained by weak tropospheric wavedriving and a series of downward wave coupling events, followed by a reflective configuration where it remained almost undisturbed until April 2020 [Lawrence et al., 2020]. The strength of the SPV was shown by the zonal wind anomalies. In MUAM, the zonal wind throughout JFM 2020 showed positive anomalies in troposphere and stratosphere, but negative anomalies in the USLM where not visible as they were in MERRA-2 data. Due to nudging, the MUAM output up to 10 hPa fits the MERRA 2 data better. Quantitatively however, the zonal wind anomalies are still underestimated compared to MERRA 2 reanalysis data. Because only monthly means were used in MUAM, a direct comparison is difficult. Furthermore, a different reference period was used to calculate the anomalies. For a better investigation of atmospheric processes, higher temporal resolution should be applied.

To quantify wave driving, EP flux was calculated from MUAM data. Despite the limitation due to monthly means, the results depicted the main wave propagation processes quite well. Due to the short livedness of wave reflection and downward coupling events, single events cannot be seen in the monthly means. Noticeable in the 2019/20 NH winter was also the strong coupling between the stratospheric NAM and the tropospheric AO as shown above. The tropospheric AO was locked in a positive phase over months, causing arctic SLP to be anomalously low throughout the winter months. This and the anomalies in the near surface windfield were visible in the monthly MUAM means. But again, this is mainly due to the usage of reanalysis data in these height levels.

References

- [1] Lawrence, Z.D., Perlwitz, J., Butler, A., Manney, G.L., Newman, P.A., Lee, S.H., Nash, E.R.: The remarkably strong Arctic stratospheric polar vortex of winter 2020: Links to record-breaking Arctic Oscillation and ozone loss. *Journal of Geophysical Research: Atmospheres*, 125, e2020JD033271. <https://doi.org/10.1029/2020JD033271>, 2020.
- [2] Overland, J. and Wang, M.: The 2020 Siberian heat wave. *International Journal Climatology*, DOI: 10.1002/joc.6850, 2020.
- [3] Ciavarella, A., Cotterill, D., Stott, P. (2020, July 15). Siberian heatwave of 2020 almost impossible without climate change. world weather attribution. <https://apastyle.apa.org/blog/two-reference-formats>
- [4] Pogoreltsev, A. I., Vlasov, A. A., Froehlich, K., und Jacobi, C.: Planetary waves in coupling the lower and upper atmosphere, *Journal of Atmospheric and Solar-Terrestrial Physics*, 69, 2083 - 2101, doi: 10.1016/j.jastp.2007.05.014, 2007.
- [5] Lilienthal, F., Krug, A., Hellmuth, F., Cremer, R.: Dokumentation für MUAM, 2016.
- [6] Froehlich, K. and Jacobi, C.: The solar cycle in the middle atmosphere: changes of the mean circulation and of propagation conditions for planetary waves , *Wiss. Mitt. Inst. f. Meteorol. Univ. Leipzig*, [www.uni-leipzig.de/ jacobi/docs/2004 LIM 1.pdf](http://www.uni-leipzig.de/jacobi/docs/2004_LIM_1.pdf), 2004.
- [7] Froehlich, K., Pogoreltsev, A., und Jacobi, C.: 161 - 189 The 48 Layer COMMA-LIM Model: Model description, new Aspects, and Climatology, *Wiss. Mitt. Inst. f. Meteorol. Univ. Leipzig*, 2003.
- [8] Charney, J. G. and Drazin, P. G.: Propagation of planetary-scale disturbances from the lower into the upper atmosphere. *Journal of Geophysical Research*, 66(1), 83–109. <https://doi.org/10.1029/JZ066i001p00083>, 1961.
- [9] Dunn-Sigouin, E. and Shaw, T. A.: Comparing and contrasting extreme stratospheric events, including their coupling to the tropospheric circulation. *Journal of Geophysical Research: Atmospheres*, 120, 1374–1390. <https://doi.org/10.1002/2014JD022116>, 2015.
- [10] Shaw, T. A. and Perlwitz, J.: The life cycle of Northern Hemisphere downward wave coupling between the stratosphere and troposphere. *Journal of Climate*, 26(5), 1745–1763. <https://doi.org/10.1175/JCLI-D-12-00251.1>, 2013.
- [11] Kidston, J., Scaife, A. A., Hardiman, S. C., Mitchell, D. M., Butchart, N., Baldwin, M. P., Gray, L. J.: Stratospheric influence on tropospheric jet streams, storm tracks and surface weather. *Nature Geoscience*, 8(6), 433–440. <https://doi.org/10.1038/ngeo2424>, 2015.

-
- [12] Domeisen, D. I. V.: Estimating the frequency of sudden stratospheric warming events from surface observations of the North Atlantic Oscillation. *Journal of Geophysical Research: Atmospheres*, 124, 3180–3194. <https://doi.org/10.1029/2018JD030077>, 2019.
- [13] Baldwin, M. P. and Dunkerton, T. J.: Stratospheric harbingers of anomalous weather regimes. *Science*, 294(5542), 581–584. <https://doi.org/10.1126/science.1063315>, 2001.

List of Figures

- 1 *ERA5 near surface temperature (T_{2m}) anomalies [$^{\circ}C$] for Jan-Jun 2020. Reference period: 1981-2010. Cited from Ciavarella et al. (2020). III*
- 2 *Time series of zonal mean zonal wind anomalies as a function of latitude at 10 hPa (a) and at $60^{\circ}N$ as a function of pressure (b). The gray line contours represent the climatology; the black lines enclose the times when anomalies exceed +2 standard deviations of the November–April daily climatology; and stippling indicates when the zonal wind values were maxima in the MERRA-2 record. Cited from Lawrence et al. (2020). The red box in both figures was added later and marks the height and time spans both figures show to make comparison easier. VI*
- 3 *Monthly zonal mean zonal wind anomalies JFM 2020 based on the JFM 2008-2018 means. Computed with MUAM. VI*
- 4 *EP flux (red arrows) and its divergence (contours) of February 2020 as function of pressure and latitude, calculated with MUAM. Blue lines show the mean zonal wind in m/s. VII*
- 5 *EP flux anomalies (red arrows) and its divergence anomalies (contours) of February 2020 as function of pressure and latitude. Reference period is the 2008-2018 February mean. VII*
- 6 *Time series of the Northern Annular Mode (a) and CPC Arctic Oscillation (b) indices from November 2019 through April 2020 Cited from Lawrence et al. (2020). VIII*
- 7 *850 hPa geopotential height anomalies (left) and 850 hPa meridional wind anomalies (right) in February 2020, calculated with MUAM. Reference periode was 2008-2018. VIII*
- 8 *Maps of the observed January–March (JFM) 2020 anomalies in surface temperature (a), and the anomalies congruent with the JFM AOCPC (b). Cited from Lawrence et al. (2020). IX*